

Supplemental information

**Oncolytic virus-driven immune remodeling
revealed in mouse medulloblastomas
at single cell resolution**

Jack Hedberg, Adam Studebaker, Luke Smith, Chun-Yu Chen, Jesse J. Westfall, Maren Cam, Amy Gross, Ilse Hernandez-Aguirre, Alexia Martin, Doyeon Kim, Ravi Dhital, Yeaseul Kim, Ryan D. Roberts, Timothy P. Cripe, Elaine R. Mardis, Kevin A. Cassady, Jeffrey Leonard, and Katherine E. Miller

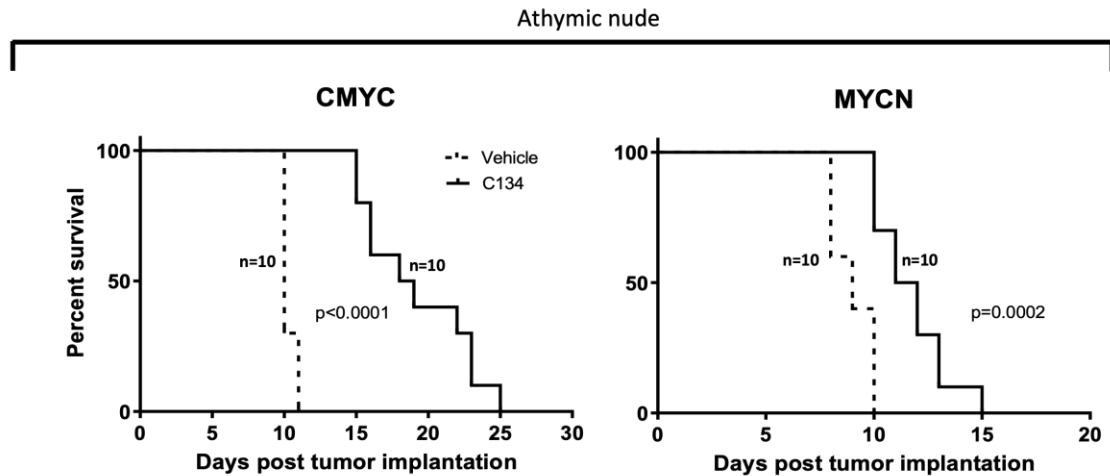


Fig. S1. Survival Study of C134 Treatment in Athymic Nude Murine Models of Medulloblastoma. Medulloblastoma tumors were established in the right cerebral cortices of T cell deficient athymic nude mice. Five days after tumor implantation, the mice received 1×10^7 pfu of C134. Mice treated with C134 had significantly longer survival times than mice receiving vehicle only. Kaplan-Meier curves depict differences in survival and statistical differences determined using the log-rank test.

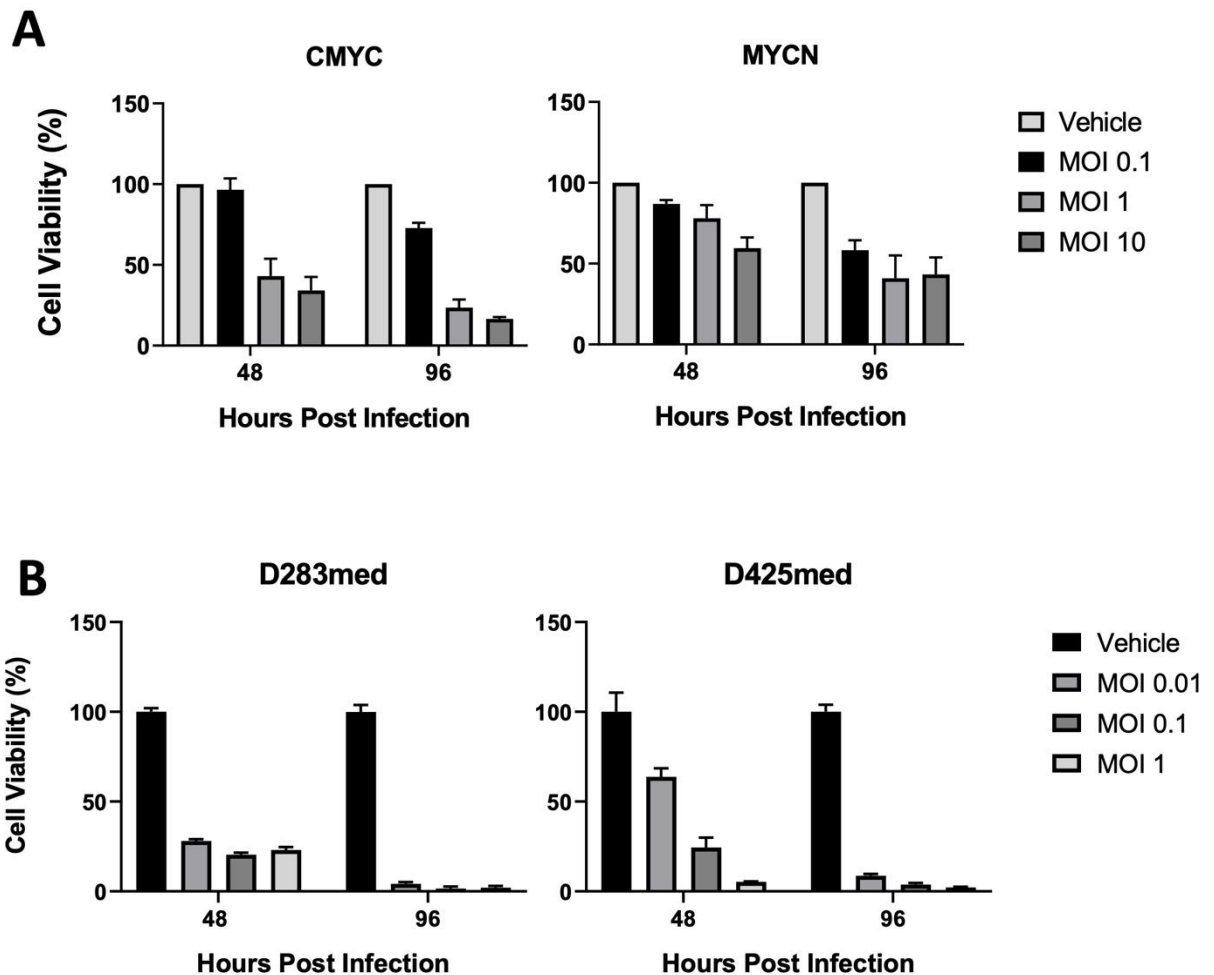


Fig. S2. Murine and Human Medulloblastoma Sensitivity to C134. Viabilities of murine (A) and human (B) medulloblastoma cell cultures were determined following C134 administration. (A) The viability of CMYC and MYCN following administration of C134 at a MOI = 0.1, 1, and 10. (B) The viability D283med and D425med following administration of C134 at a MOI = 0.01, 0.1, and 1. For all experiments, the number of viable cells was determined at 48 and 96 hours post infection and normalized against the number of mock-infected cells. Means + SEM are shown (n = 8).

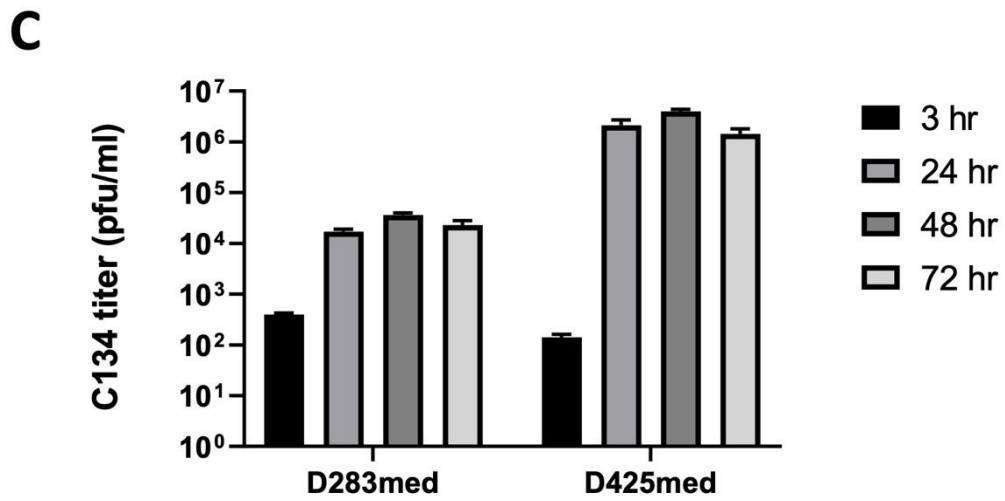
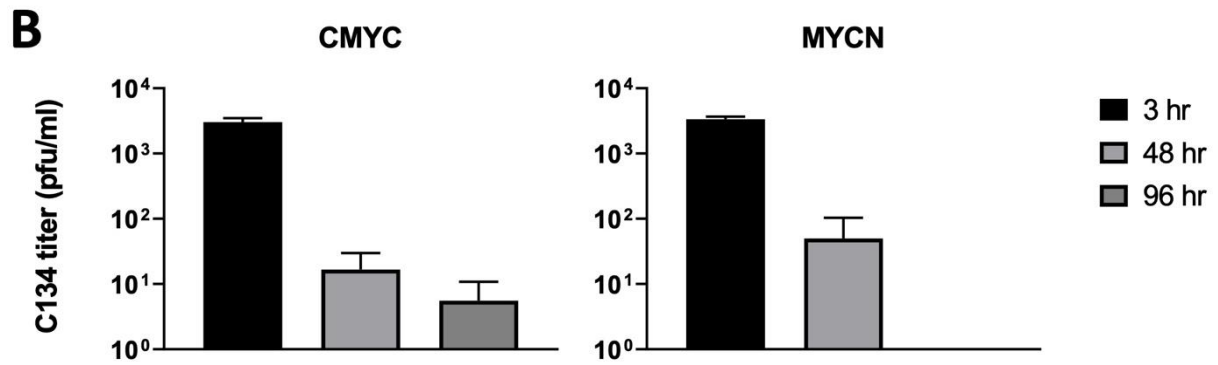
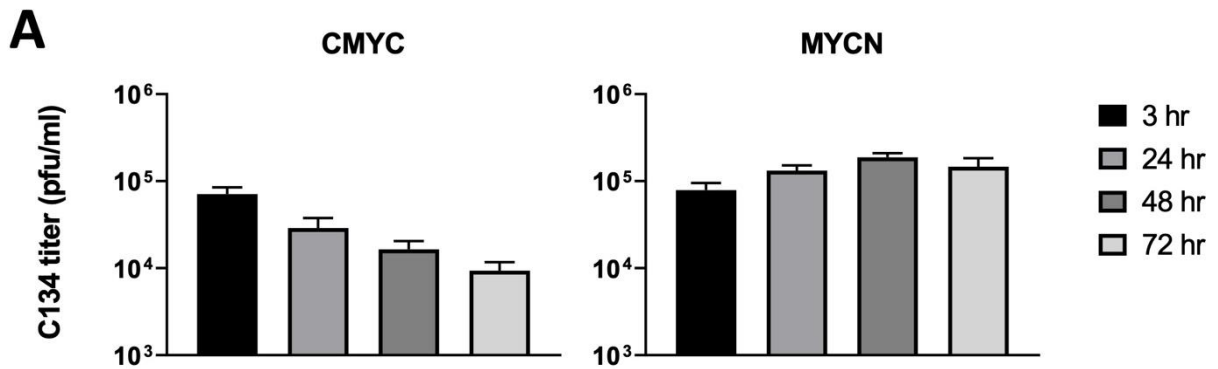


Fig. S3. Amount of C134 Recoverable from Murine and Human Medulloblastoma. (A)

Amount of C134 recoverable from murine medulloblastoma cell cultures assessed by titers obtained following infection at a MOI = 1. Cells and supernatants were collected at the times designated and virus titers determined by standard plaque assays on Vero cells. Means + SEM are shown (n = 3 biological replicates performed in triplicate). **(B)** Amount of C134 recoverable from murine medulloblastoma tumors assessed by titers obtained following intra-tumoral administration of 1×10^7 pfu. Brain tumor quadrants were harvested at the times designated and virus titers determined by standard plaque assays on Vero cells. Means + SEM are shown (n = 4 biological replicates performed in triplicate). **(C)** Amount of C134 recoverable from human medulloblastomas assessed by titers obtained following infection at a MOI = 0.01. Cells and supernatants were collected at the times designated and virus titers determined by standard plaque assays on Vero cells. Means + SEM are shown (n = 3 biological replicates performed in triplicate).

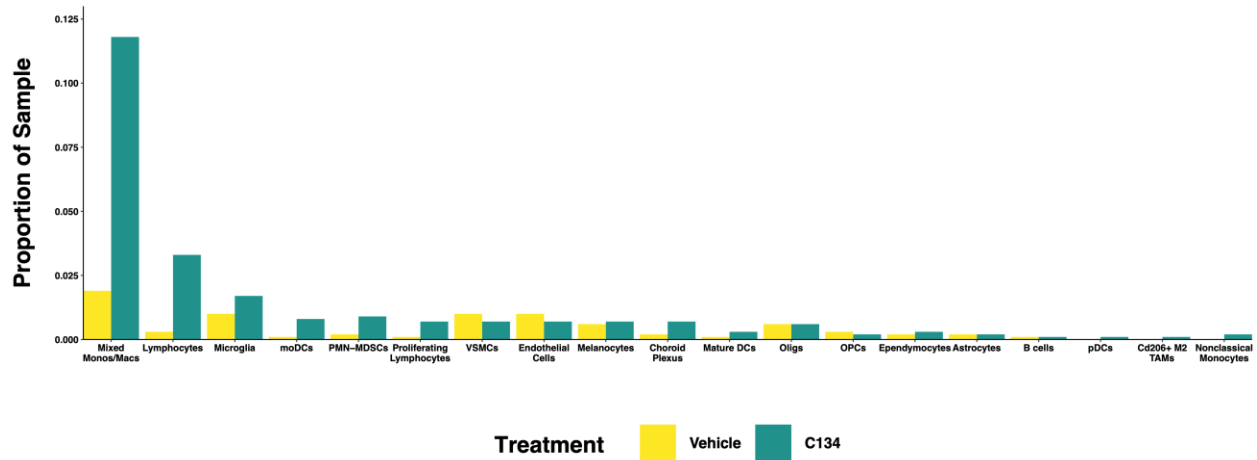


Fig. S4. Proportions of scRNA-Seq Samples Occupied by Cell Types Annotated From Immune Cell Subset Split by Treatment Status. Medulloblastoma cells are omitted to show differences in all other cell types.

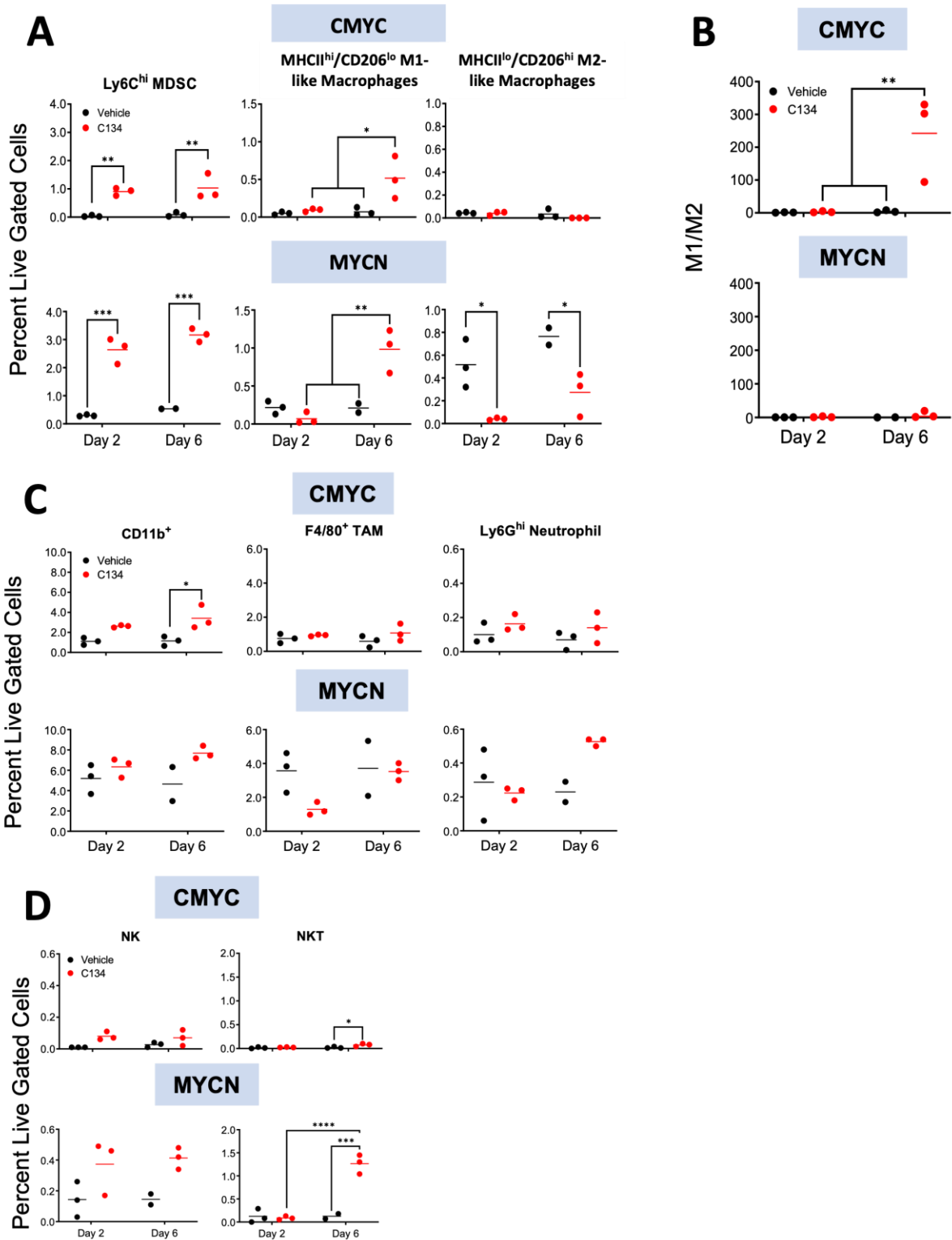


Fig. S5. C134 Treatment Effect on Innate Immune Infiltrate and MDSCs. Flow cytometry quantification of MDSC and macrophage immune infiltrate (A), ratio of M1-like Macrophages to

M2-like macrophages (**B**), tumor-associated macrophage and neutrophil infiltrate (**C**), and NK and NKT infiltrate (**D**) in CMYC and MYCN tumors two- and six-days post C134 or vehicle administration. Statistical analysis was performed using two-way ANOVA Tukey's multiple comparisons test (* $p < 0.05$, ** $p < 0.01$, *** $p < 0.001$ and **** $p < 0.0001$).

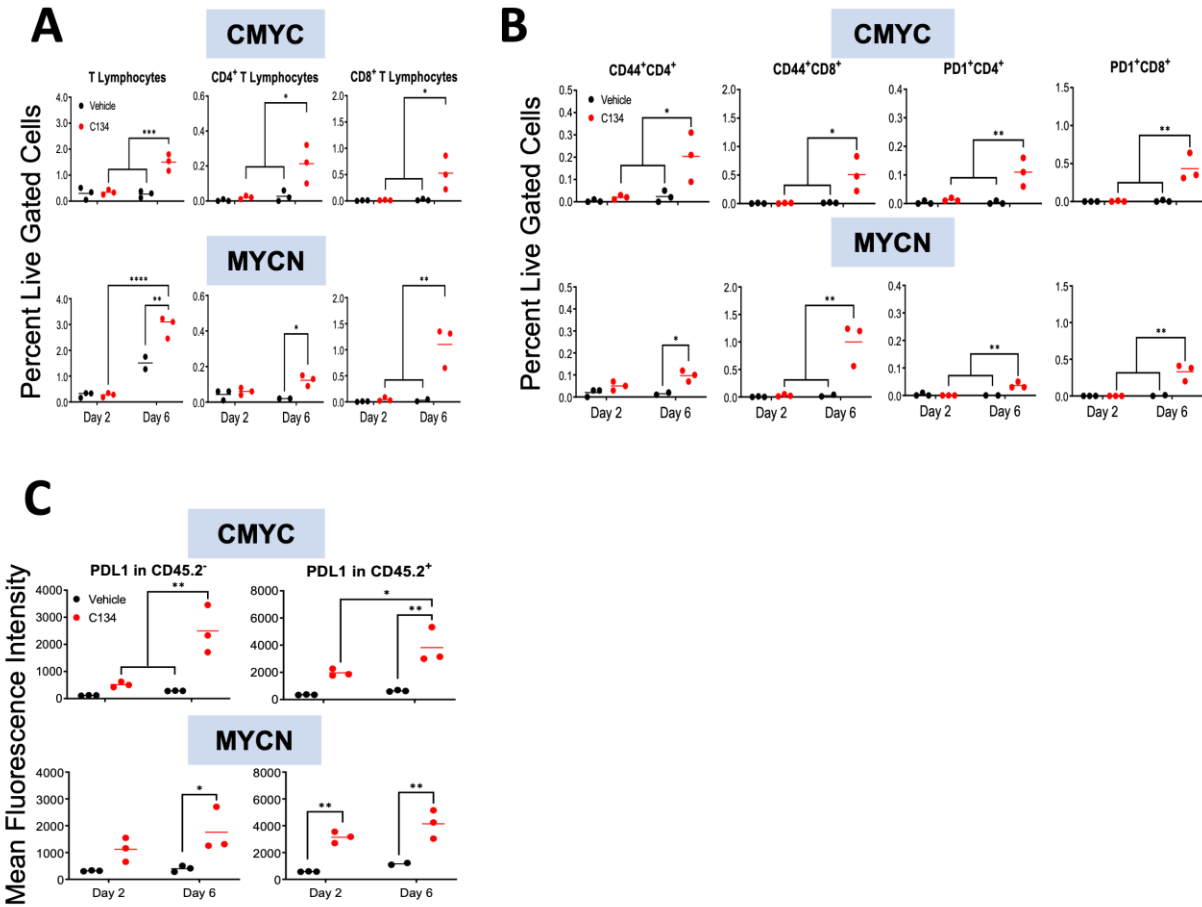


Fig. S6. C134 Treatment Effect on T Cell Infiltrate and Immune Checkpoint Molecules.

Flow cytometry quantification of CD4⁺ and CD8⁺ T lymphocyte infiltrate (**A**), CD44⁺ T cells and PD1⁺ T cells (**B**), and PDL1⁺ cells in CD45.2⁻ and CD45.2⁺ populations (**C**) in CMYC and MYCN tumors two- and six-days post C134 administration. Statistical analysis was performed using two-way ANOVA Tukey's multiple comparisons test (* $p < 0.05$, ** $p < 0.01$, *** $p < 0.001$ and **** $p < 0.0001$).

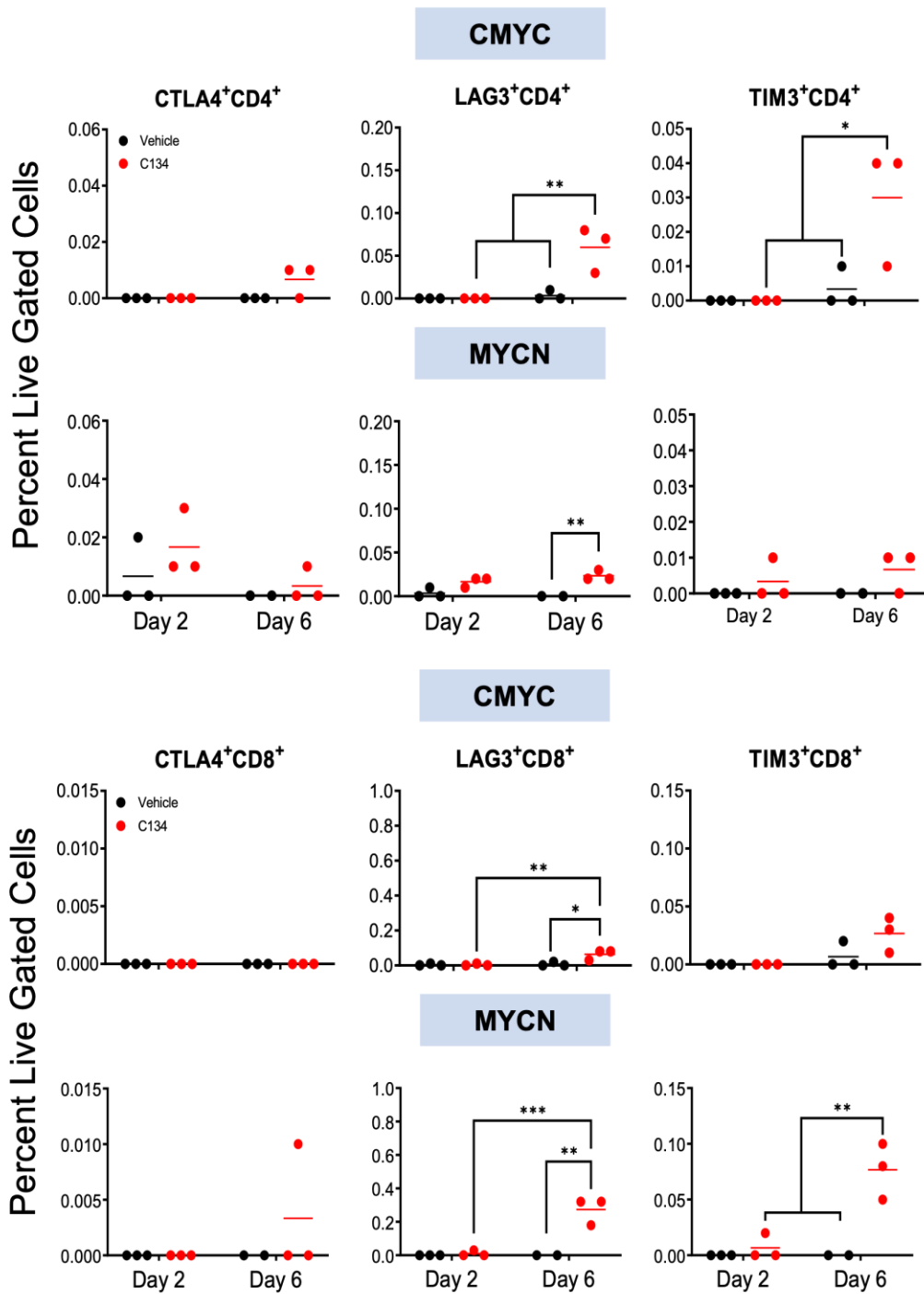


Fig. S7. Quantification of Immune Checkpoint Molecules Following C134 Treatment. Flow cytometry quantification of immune checkpoint molecules on tumor lymphocyte infiltrates in CMYC and MYCN tumors two- and six-days post C134 administration. Statistical analysis was

performed using two-way ANOVA Tukey's multiple comparisons test (* $p < 0.05$, ** $p < 0.01$, *** $p < 0.001$ and **** $p < 0.0001$).

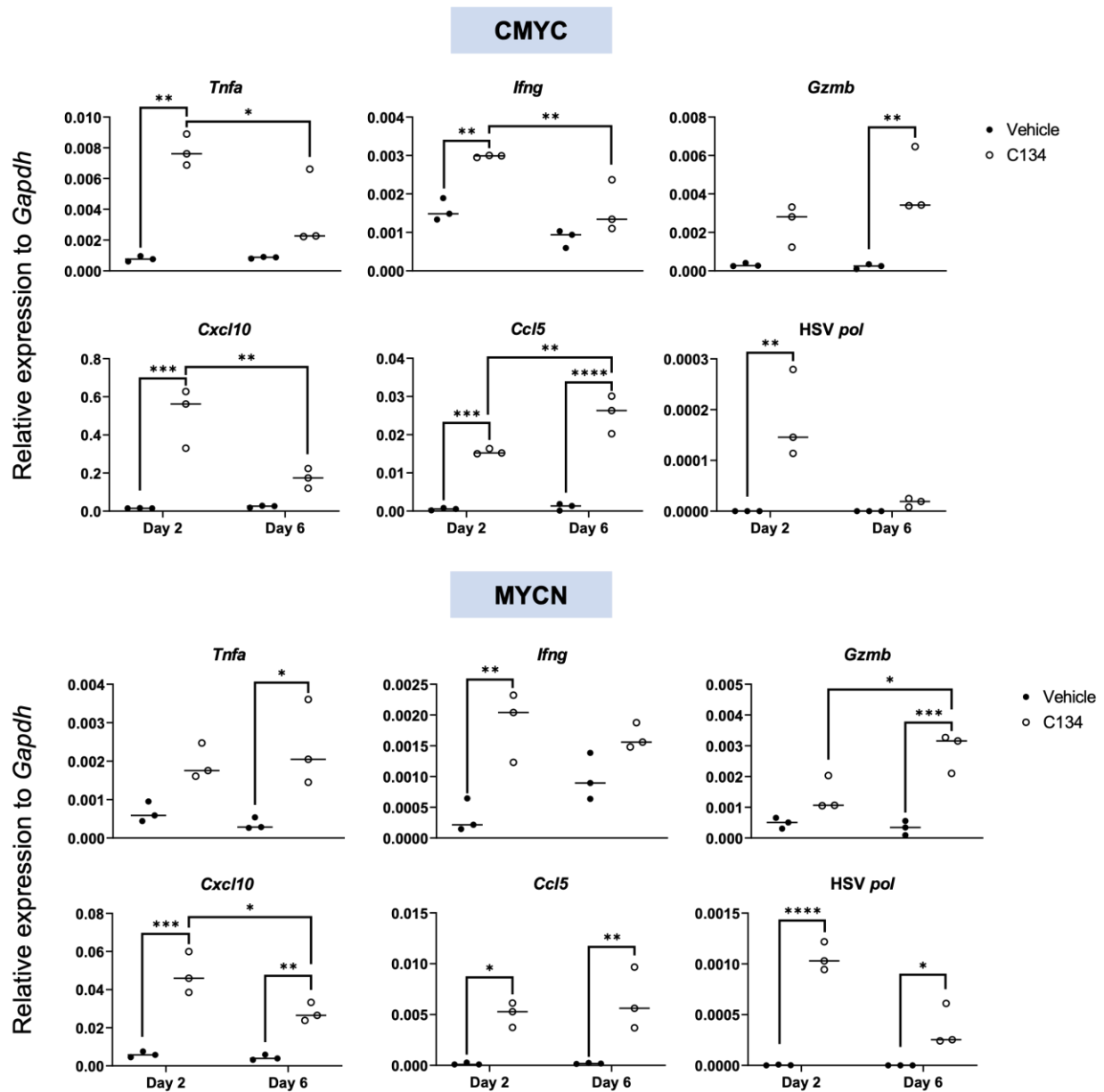


Fig. S8. Quantitative PCR of Inflammatory and C134 Gene Expression in Mouse

Medulloblastomas. CMYC and MYCN tumors were harvested two- and six-days post C134

administration. Pro-inflammatory and immune-stimulating genes were evaluated using

quantitative real-time PCR analysis. Statistical analysis was performed using two-way ANOVA

Tukey's multiple comparisons test (* $p < 0.05$, ** $p < 0.01$, *** $p < 0.001$ and **** $p < 0.0001$).

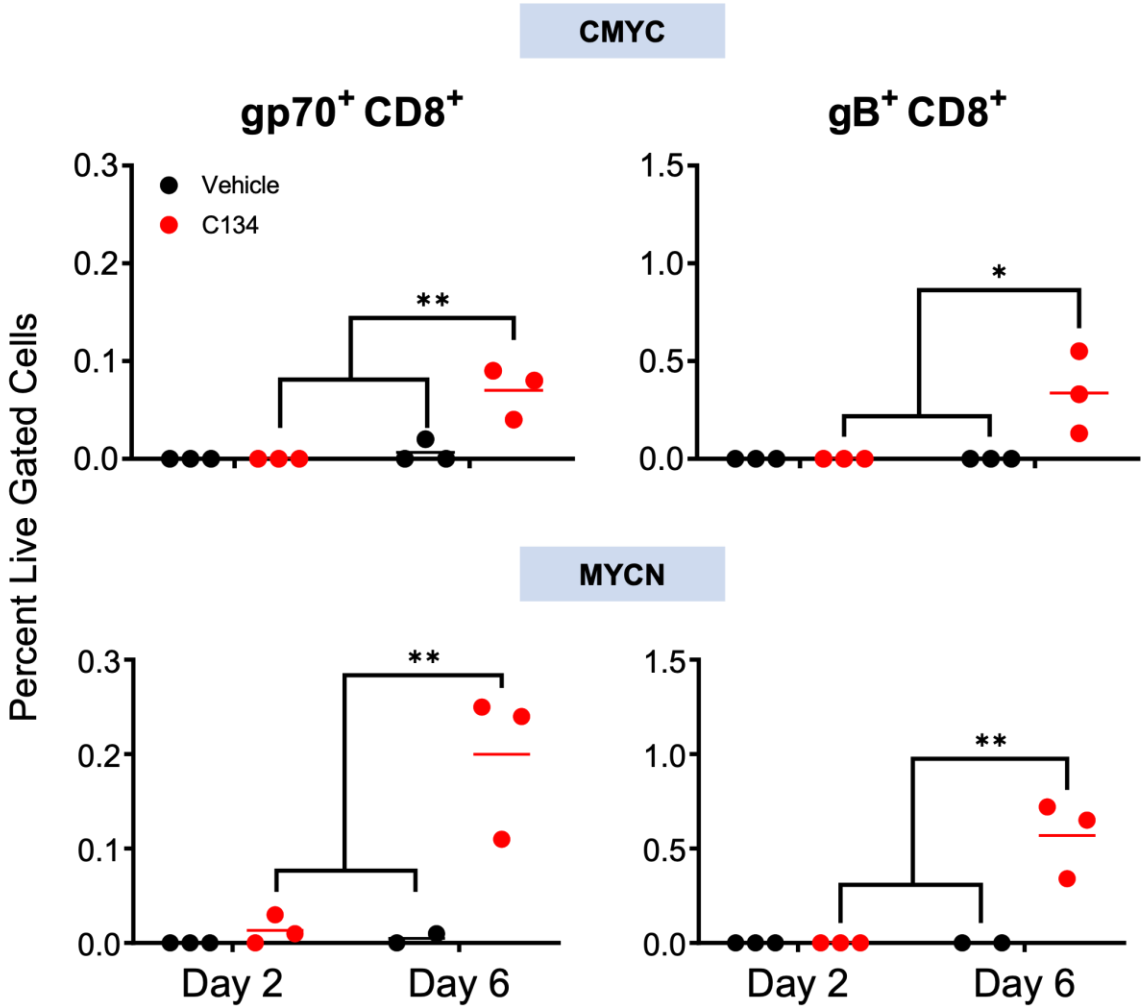


Fig. S9. Virus and Mouse Antigen T Cell Specificity Following C134 Treatment. Flow cytometry quantification of CD8⁺ T cell antigen specificity in CMYC and MYCN tumors two- and six-days post C134 administration. Statistical analysis was performed using two-way ANOVA Tukey's multiple comparisons test (*p < 0.05, **p < 0.01, ***p < 0.001 and ****p < 0.0001).

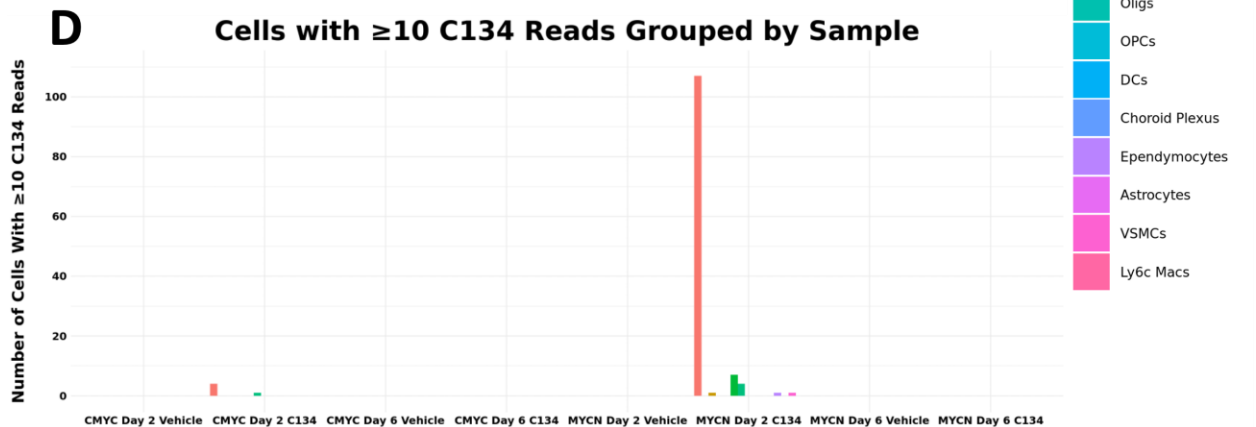
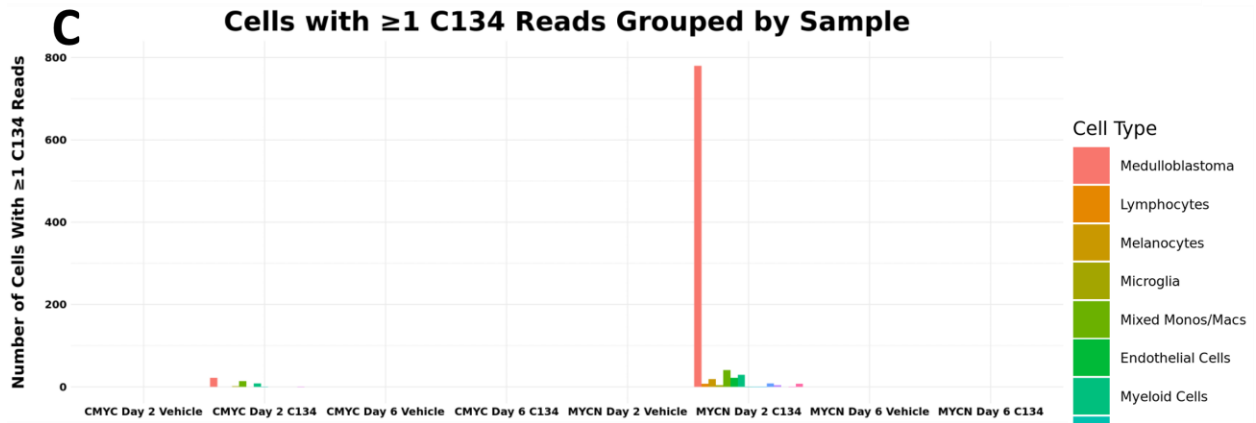
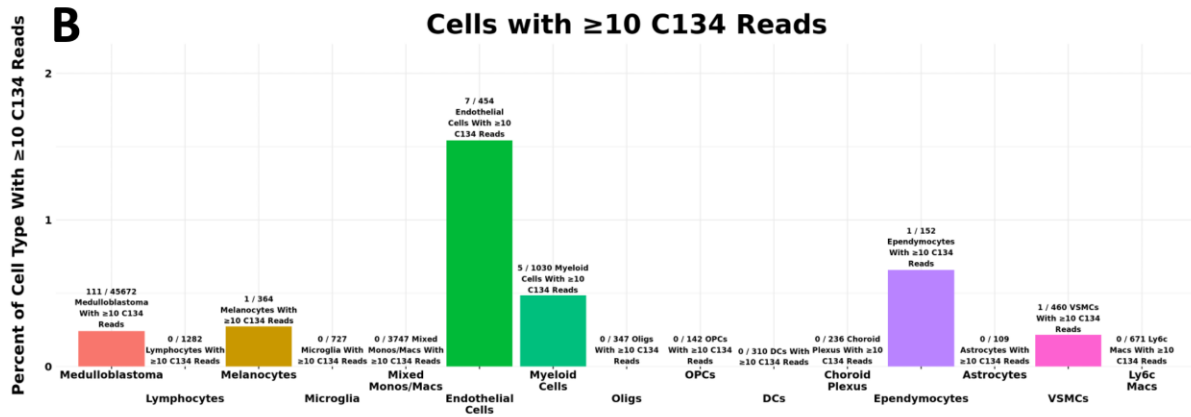
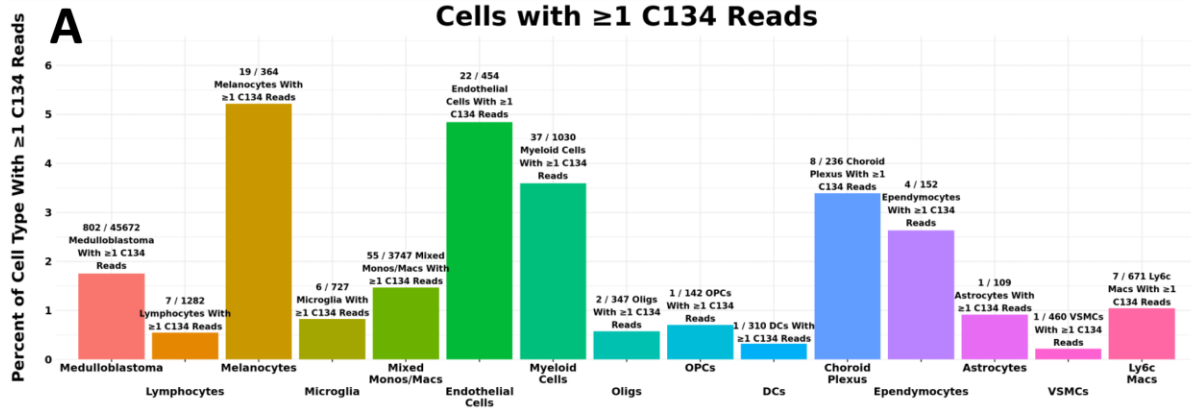
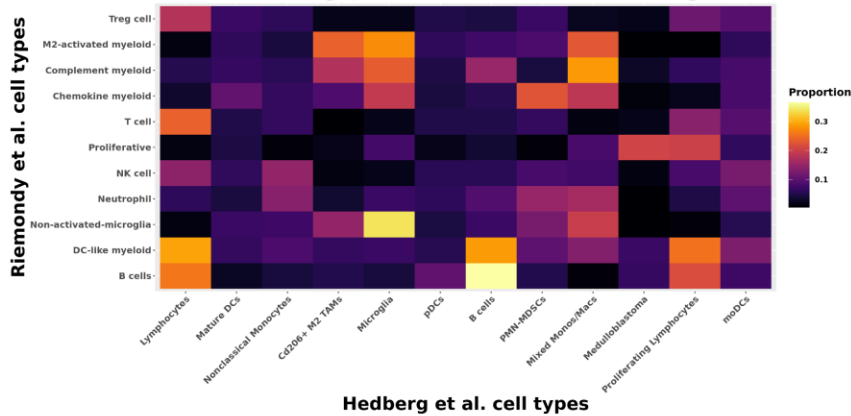


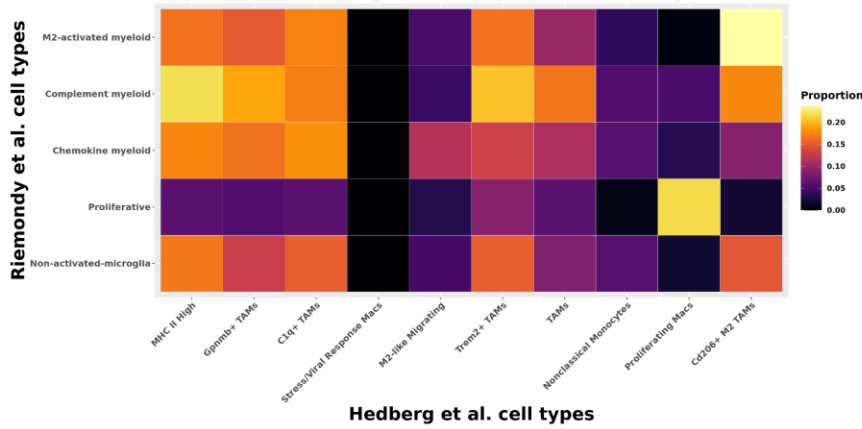
Fig. S10. Quantification of Cell Types With C134 Reads in Single Cell RNA Sequencing

Data. Depicted are overall percentages of cells by cell type with greater than or equal to 1 read aligning to C134 (A), or greater than or equal to 10 reads aligning to C134 (B). Y axes depict percentages while text above individual bars depicts absolute numbers of cells in each cell type meeting the respective thresholds of reads aligning to C134. (C) and (D) depict absolute numbers of cells containing greater than or equal to 1 read aligning to C134 (C) or greater than or equal to 10 reads aligning to C134 (D) across samples and cell types.

A Overlap in Top 200 Marker Genes Per Immune Cell Type with Riemondy et al.



B Overlap in Top 200 Marker Genes Per Macrophage Subset Cell Type with Riemondy et al.



C

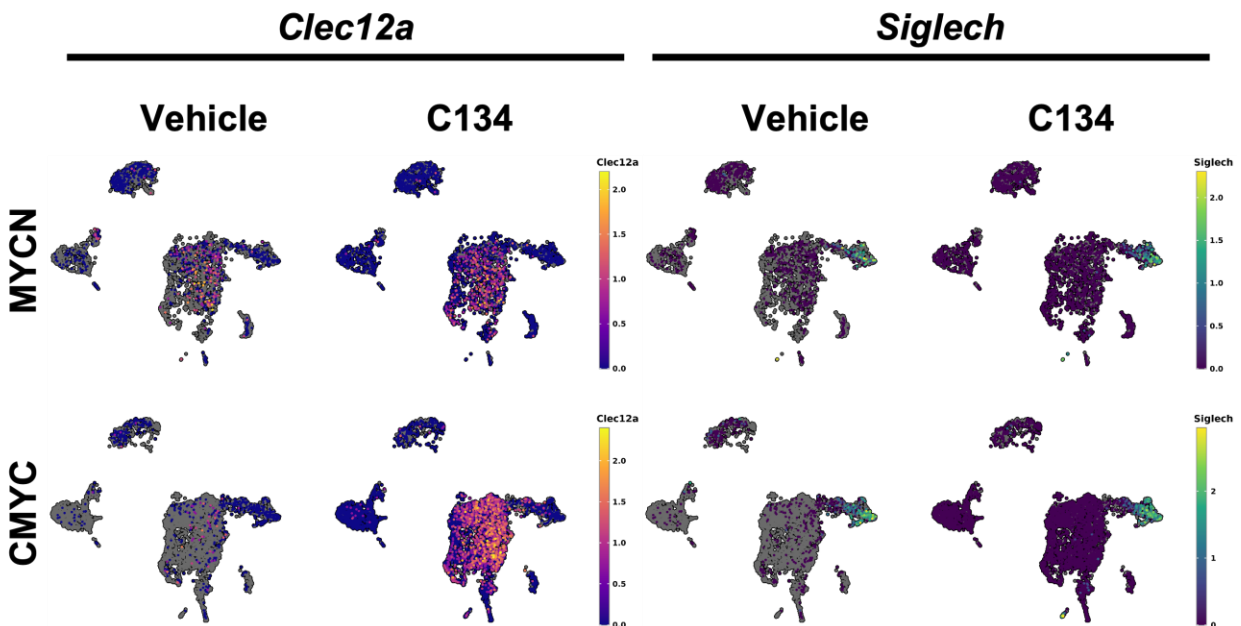
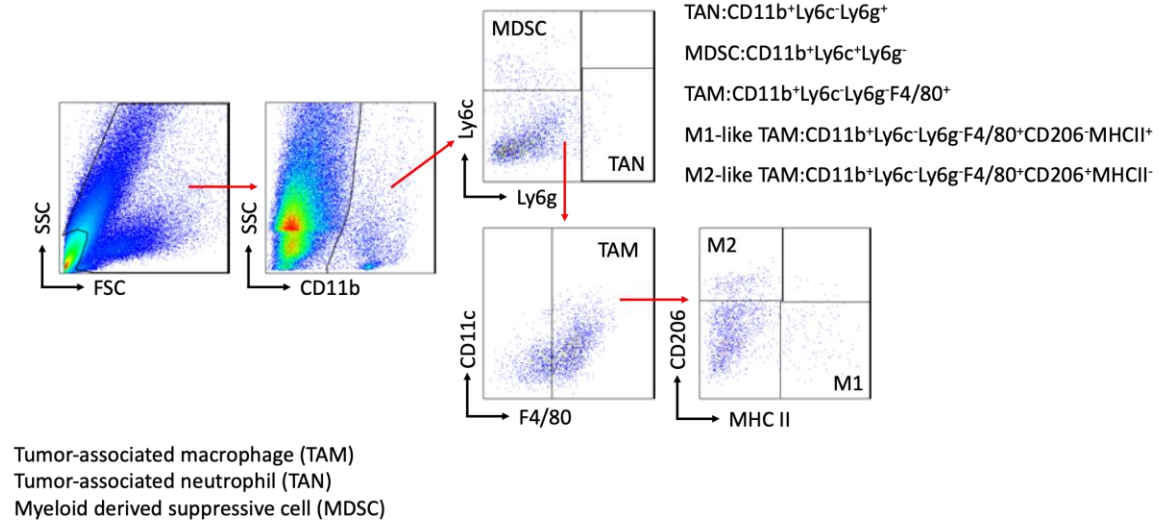


Fig. S11. Comparative Analyses With Other Medulloblastoma Immune Studies. Top cell type/cluster marker genes were obtained from supplementary table 7 of Riemond et al. and read into R. Genes with adjusted p-values < 0.05 were then filtered, arranged by their logFC, and the top 200 genes with greatest logFC for each cell type were extracted. The gene symbols were then converted into mouse orthologs using the orthologsBioMART package. Subsequently, the top 200 immune cell subset marker genes from this study for each cell type were extracted, and represented above are the proportion of genes for each Riemond et al. cell type independently identified in the top 200 marker genes for each immune cell subset cell type (A) and each macrophage subset cell type (B) in the present study. Shown in (C) are UMAPs of medulloblastoma immune cell subsets split by treatment group and medulloblastoma model, illustrating the normalized expression of the Clec12a and Siglech genes, identified by Dang et al. as indicative of monocyte-derived cells and microglia, respectively.

A

Gating strategy for myeloid cell populations



B

Gating strategy for lymphocytes

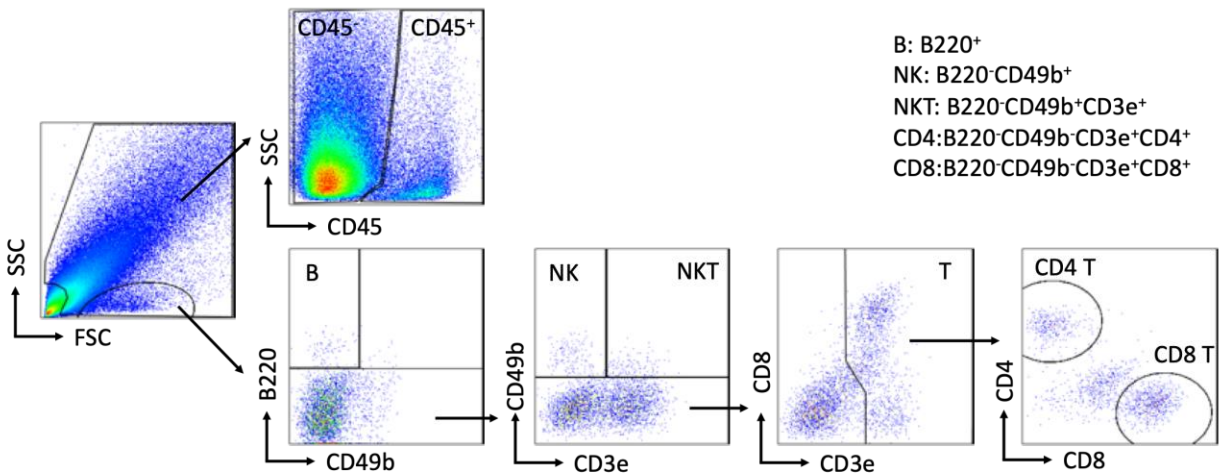


Fig. S12. Flow Cytometry Gating Strategies. Myeloid cell population (A) and lymphocyte (B)

gating strategies are shown.

Table S1. Single Cell Sequencing Quality Control and Differential Gene Expression Data.

This table contains tabs that contain quality control metrics for single cell RNA sequencing data described in this paper. Additional tabs contain data outputs from differential gene expression analysis identifying cluster markers, cell type markers, and differentially expressed genes for the treatment groups, timepoints, medulloblastoma models, and cells with C134 reads detected, corresponding to the figure panels to which tab titles refer.